nature genetics

Recurrent inactivating *RASA2* mutations in melanoma

Rand Arafeh[1], Nouar Qutob[1], Rafi Emmanuel[1], Alona Keren-Paz[1], Jason Madore[2,3], Abdel Elkahloun[4], James S Wilmott[2,3], Jared J Gartner[5], Antonella Di Pizio[6], Sabina Winograd-Katz[1], Sivasish Sindiri[5], Ron Rotkopf[7], Ken Dutton-Regester[8], Peter Johansson[8], Antonia L Pritchard[8], Nicola Waddell[8], Victoria K Hill[4], Jimmy C Lin[5], Yael Hevroni[1], Steven A Rosenberg[5], Javed Khan[5], Shifra Ben-Dor[7], Masha Y Niv[6], Igor Ulitsky[9], Graham J Mann[2,3,10], Richard A Scolyer[2,3,11], Nicholas K Hayward[8] & Yardena Samuels[1]

Analysis of 501 melanoma exomes identified *RASA2*, encoding a RasGAP, as a tumor-suppressor gene mutated in 5% of melanomas. Recurrent loss-of-function mutations in *RASA2* were found to increase RAS activation, melanoma cell growth and migration. RASA2 expression was lost in ≥30% of human melanomas and was associated with reduced patient survival. These findings identify *RASA2* inactivation as a melanoma driver and highlight the importance of RasGAPs in cancer.

Cutaneous melanoma, for which incidence rates continue to increase[1], represents a major health problem worldwide. Recent genomic studies of melanoma[2–4] have discovered several driver genes and enabled the development of targeted drugs, which show promise in treating patients with melanoma[5,6]. However, responses to these drugs are rarely durable; therefore, there is an urgent need to identify additional targetable alterations in melanoma.

Most approved drugs that target genetically altered proteins in cancer are to kinases[7]. However, a majority of the proteins mutated in cancer are tumor suppressors, which cannot be reactivated by small molecules. A possible solution involves exploiting the fact that tumor-suppressor gene inactivation results in activation of a downstream growth pathway. For example, *PTEN* mutations lead to increased activity of the downstream kinase AKT[8]. In this study, we sought to systematically identify tumor-suppressor genes involved in melanoma and characterize the downstream pathways activated by their loss of function.

We compiled somatic mutation data from the whole-exome (465 samples) and whole-genome (36 samples) sequences of 501 melanomas from various sources, including The Cancer Genome Atlas (TCGA)[2,3]. Data were analyzed as described previously[9] (**Supplementary Tables 1** and **2**). Genes were ranked on the basis of the frequency of nonsynonymous mutations, the number of mutations per megabase and mutation burden[9]. We then identified genes for which nonsense or frameshift mutations constituted at least 20% of all the gene's mutations, a suggested threshold for tumor-suppressor genes[10]. The highest ranking genes were *TP53*, *NF1*, *ARID2*, *CDKN2A* and *PTEN*. After these, *RASA2* was mutated in 5.4% of patients (**Table 1**), and 27% of the mutations were alterations leading to loss of function (**Table 1**). The distribution of the 32 protein alterations encoded by the nonsynonymous mutations identified in *RASA2* is shown in **Figure 1a**. We profiled the copy number landscape of 22 samples using the CytoScan High-Definition array (Affymetrix) and found three focal deletions (13.6%). Consistent with these data, examination of the copy number variation (CNV) data for the TCGA melanoma cohort showed deletions of the *RASA2* locus in 11.7% of cases. Furthermore, we found that *RASA2* was null in 1% of the melanoma samples investigated. This places *RASA2* in the top 10% of all genes, and, when considering a normalized number of losses, it is significant ($P < 0.05$). Thus, *RASA2* is a potential tumor-suppressor gene in melanoma (**Table 1**, **Supplementary Fig. 1** and **Supplementary Table 2**).

RASA2 encodes a GTPase-activating protein (GAP), which stimulates the GTPase activity of wild-type RAS but not its mutant, oncogenic form. Acting as a suppressor of RAS function, RASA2 enhances the weak intrinsic GTPase activity of RAS, resulting in the inactive, GDP-bound isoform[11]. Notably, the role of RASA2 has not previously been investigated in melanoma. Recently, *NF1*, which encodes another RAS-specific GAP, has been found to be frequently mutated and to have a central role in melanoma[2–4]. Mutations in *RASA2* and *NF1* co-occur with high significance ($P = 0.000011$, Fisher's exact test) (**Fig. 1b** and **Supplementary Table 3**), consistent with a report published while this paper was under revision[4]. Examination of publicly available

Table 1 Melanoma driver genes for which at least 20% of the identified mutations are loss of function

Gene	Percent of tumors with mutation	Percent of all coding mutations that are LOF
TP53	17.1	33.3
NF1	14.4	42.0
ARID2	12.6	53.0
CDKN2A	12.4	57.6
PTEN	8.8	44.4
SETD2	5.4	32.4
RASA2	5.4	27.3

Genes were ranked according to the frequency of nonsynonymous mutations, the number of mutations per megabase, the mutation rate (taking into account base coverage) and the presence of deleterious (nonsense or frameshift) mutations in at least 20% of the cases. LOF, loss of function.

[1]Molecular Cell Biology Department, Weizmann Institute of Science, Rehovot, Israel. [2]Melanoma Institute Australia, Sydney, New South Wales, Australia. [3]Discipline of Pathology, Sydney Medical School, University of Sydney, Sydney, New South Wales, Australia. [4]National Human Genome Research Institute, US National Institutes of Health, Bethesda, Maryland, USA. [5]National Cancer Institute, US National Institutes of Health, Bethesda, Maryland, USA. [6]Institute of Biochemistry, Food Science and Nutrition, Hebrew University, Rehovot, Israel. [7]Department of Biological Services, Weizmann Institute of Science, Rehovot, Israel. [8]QIMR Berghofer Medical Research Institute, Brisbane, Queensland, Australia. [9]Department of Biological Regulation, Weizmann Institute of Science, Rehovot, Israel. [10]Centre for Cancer Research, Westmead Millennium Institute for Medical Research, University of Sydney, Sydney, New South Wales, Australia. [11]Tissue Pathology and Diagnostic Oncology, Royal Prince Alfred Hospital, Sydney, New South Wales, Australia. Correspondence should be addressed to Y.S. (yardena.samuels@weizmann.ac.il).

Received 1 June; accepted 29 September; published online 26 October 2015; doi:10.1038/ng.3427

databases demonstrated that *RASA2* is mutated in several other tumor types (**Supplementary Fig. 2**).

To test whether *RASA2* is a tumor suppressor in melanoma, we knocked down *Rasa2* expression in immortalized, non-tumorigenic mouse NIH3T3 cells, using two short hairpin RNA (shRNA) constructs. *Rasa2* knockdown resulted in RAS activation (**Supplementary Fig. 3a**), leading to increased cell growth on plastic and in soft agar (**Supplementary Fig. 3b**).

To characterize the tumorigenic effects of RASA2 inactivation in melanoma cells, we functionally characterized two recurrent *RASA2* mutations, encoding p.Arg310*, which causes RASA2 truncation, and p.Ser400Phe mapping to the catalytic RasGAP domain. We established pooled clones stably transduced with vector control or vector expressing wild-type or mutant RASA2 of the human melanoma cell lines A375 (BRAF V600E, wild-type NRAS, mutant NF1), 501Mel (BRAF V600E, wild-type NRAS, wild-type NF1), 108T (wild-type BRAF, wild-type NRAS, mutant NF1) and 55T (wild-type BRAF, wild-type NRAS, mutant NF1), which all express wild-type RASA2. We detected similar levels of overexpressed RASA2 protein in stable clones from the A375, 501Mel, 108T and 55T cell lines except for the Arg310* mutant in 108T cells, which had increased protein expression (**Supplementary Fig. 4**). These clones were used for subsequent studies.

Because *RASA2* encodes a RasGAP, we hypothesized that *RASA2* mutation or loss would alleviate RAS suppression. Indeed, modeling the effects of the RASA2 alterations on the structure of p120^{GAP} (ref. 12) predicted that the RASA2 Arg310* mutant is unable to bind to RAS,

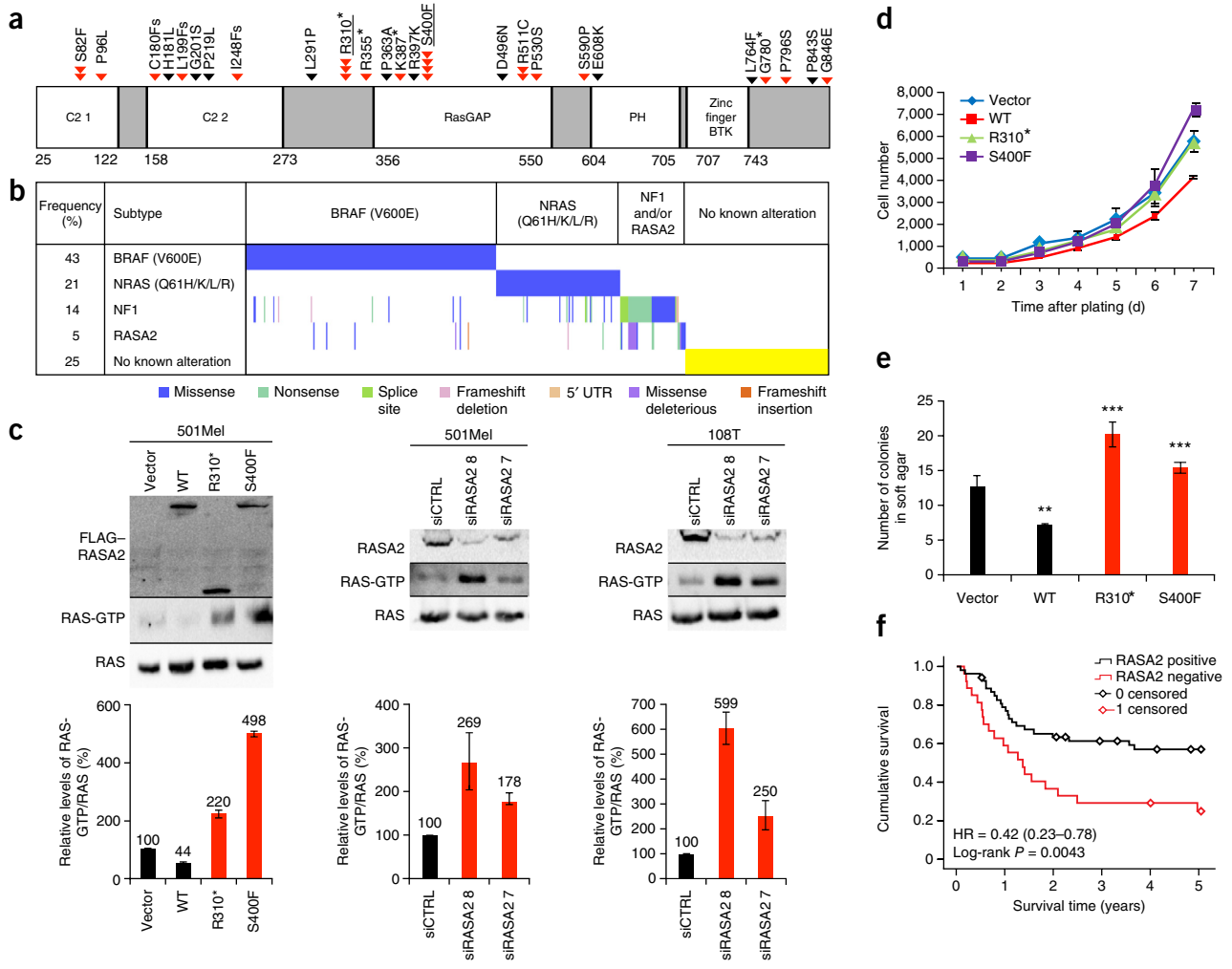

Figure 1 Effects of *RASA2* mutations on RAS activity, melanoma cell growth and patient survival. (**a**) The human RASA2 protein, with conserved domains indicated as blocks, including the C2 domain first repeat (C2 1), the C2 domain second repeat (C2 2), the RAS GTPase-activating domain (RasGAP), the Plekstrin homology domain (PH) and Bruton's tyrosine kinase cysteine-rich motif (BTK). Somatic alterations are represented by arrowheads and amino acid changes. Red triangles represent deleterious alterations. Underlined alterations were functionally assessed. (**b**) Distribution of the somatic alterations encoded in *BRAF*, *NRAS*, *NF1* and *RASA2* in melanomas ($n = 501$). (**c**) Left, immunoblot of RAS-GTP levels in 501Mel cells expressing the indicated constructs; WT, wild type. 501Mel cells (middle) and 108T cells (right) were depleted for RASA2 using small interfering RNAs (siRNAs) targeting human *RASA2* (siRASA2 8 and siRASA2 7). RAS-GTP levels were assessed by RAS pulldown assay, and the RAS-GTP/RAS ratios from two independent experiments were calculated and normalized to the ratio from vector control (siCTRL) (bottom). Error bars, s.d. (**d**) 501Mel clones expressing the indicated constructs were seeded in 96-well plates in medium with 2.5% FBS, and average cell number was measured by assessing DNA content using SYBR Green I in two independent experiments with six replicates each. Error bars, s.d. (**e**) The anchorage-independent proliferation of 501Mel clones expressing the indicated RASA2 constructs was assessed by measuring colony formation in soft agar in medium with 2.5% serum in two independent experiments with four replicates each 7 d after plating. $^{**}P < 0.005$ for wild-type RASA2 versus vector; $^{***}P < 0.0001$ for wild-type RASA2 versus the RASA2 mutants (Student's *t* tests). (**f**) Kaplan-Meier curve showing the overall survival of patients with AJCC stage III melanoma with positive ($n = 54$) or negative ($n = 27$) RASA2 expression (log-rank $P = 0.0043$).

as it lacks the RasGAP, PH and BTK domains. Although the RASA2 Ser400Phe mutant is expected to bind to RAS, the substitution is likely to affect the stabilization of the catalytic site, which may disturb structural changes necessary for GAP catalysis, leading to increased RAS activity (**Supplementary Fig. 5**). To test the effects of RASA2 on RAS, we conducted both gain- and loss-of-function studies. Overexpression of wild-type RASA2 substantially suppressed RAS-GTP levels; in contrast, both RASA2 mutants failed to suppress RAS-GTP levels, demonstrating that the two underlying mutations result in a clear loss of function (**Fig. 1c** and **Supplementary Fig. 6a**). The mutants were not found to have this effect in A375 cells owing to the high BRAF activity in these cells. This result is consistent with previous data indicating that, above a certain threshold of active protein, RAS carries out maximal pathway activation[13]. The A375 clones were therefore not analyzed further in this study. Conversely, among the melanoma cell lines that retained RASA2 expression, RNA interference (RNAi)-mediated suppression of *RASA2* led to the activation of RAS in 501Mel and 108T cells (**Fig. 1c**, middle and right). Endogenous RASA2 in 55T cells was barely detectable by immunoblotting (**Supplementary Fig. 4b**); for this reason, we did not perform *RASA2* knockdown in this cell line. Notably, reintroduction of wild-type RASA2 in melanoma cell lines that harbored *RASA2* mutations (76T (p.Arg310*) and C084 (p.Ser400Phe)) inhibited RAS activation (**Supplementary Fig. 6b**). These data confirm that RASA2 is a functional RasGAP and that mutation or loss of *RASA2* activates RAS in melanoma. The variation seen in the effects of the RASA2 mutants on RAS-GTP levels is probably due to differences in mutational background and variation in endogenous RASA2 protein abundance among the cell lines, as these factors can modulate RAS complex formation and are important in context-dependent signaling, as shown by Kiel *et al.*[14]. Furthermore, in some cases, the RASA2 mutants were found to enhance RAS-GTP levels, suggesting that the underlying variants might have dominant-negative effects. This scenario has precedent and has been described for p53 and PTEN[15,16].

To examine the effects of *RASA2* mutations on proliferation and colony-forming ability, we investigated cell growth *in vitro*. In medium containing a low concentration of serum, wild-type clones grew slower than mutant clones (**Fig. 1d** and **Supplementary Fig. 7a**). We also observed this difference in anchorage-independent cell growth, where cells expressing mutant RASA2 formed a significantly higher number of colonies than cells expressing wild-type RASA2 ($P < 0.005$, *t* test; **Fig. 1e** and **Supplementary Fig. 7c**). In agreement with the tumor-suppressor role of RASA2, overexpression of wild-type RASA2 in melanoma cell lines that harbored *RASA2* mutations (C084 and 76T) led to reduced cell growth (**Supplementary Fig. 7b**) and diminished anchorage-independent growth (**Supplementary Fig. 7c**).

As previous studies reported that the activation of RAS increases cell migration[17], we examined whether mutated RASA2 had the same effect. Expression of wild-type RASA2 in pooled 108T, 55T or 501Mel clones seeded in serum-free medium led to reduced cell migration, whereas expression of mutant RASA2 did not suppress migration ($P < 0.0001$, *t* test; **Supplementary Fig. 8**).

To validate the extent to which RASA2 protein expression is lost in human melanomas and to assess the prognostic potential of this loss, we performed RASA2 immunohistochemistry on a set of American Joint Committee on Cancer (AJCC) stage III melanomas (**Supplementary Fig. 9**)[18,19]. We found that RASA2 expression was negative in 33% (27/81) of cases and positive in 67% (54/81) of melanomas (**Supplementary Fig. 9c**). A Kaplan-Meier plot and log-rank testing showed that loss of RASA2 expression (negative by immunohistochemistry) was significantly associated with poorer survival: hazard ratio (HR) = 0.42, confidence interval (CI) = 0.23–0.78; log-rank $P = 0.0043$ (**Fig. 1f**). These results further emphasize the role of RASA2 loss in melanoma progression and indicate that it has prognostic relevance.

The finding of common alterations in *RASA2*, together with functional data indicating the effect of these alterations on cell growth and migration, suggests that *RASA2* is an important tumor suppressor in human melanoma. Particularly notable is the fact that RASA2 suppression provides an alternative mechanism of RAS activation. This study demonstrates that melanomas have somatic mutations in the *RASA2* gene that lead to impaired RASA2 activity and constitutive activation of RAS signaling.

URLs. All statistical calculations were performed in the R statistical environment, http://www.r-project.org/.

METHODS

Methods and any associated references are available in the online version of the paper.

Accession codes. Sequence data reported in this paper are available for download from dbSNP under accession 1062266.

Note: Any Supplementary Information and Source Data files are available in the online version of the paper.

ACKNOWLEDGMENTS

We thank T. Wiesel for graphical assistance. This work was supported by the Intramural Research Programs of the National Human Genome Research Institute and the National Cancer Institute, as well as by program grants of the Australian National Health and Medical Research Council (NHMRC) and Cancer Institute NSW. Y.S. is supported by the Israel Science Foundation through grants 1604/13 and 877/13, the European Research Council (ERC; StG-335377), the ERC under the European Union's Horizon 2020 research and innovation program (grant agreement *677645*), the Henry Chanoch Krenter Institute for Biomedical Imaging and Genomics, the estate of Alice Schwarz-Gardos, the estate of John Hunter, the Knell Family, the Peter and Patricia Gruber Award and the Hamburger Family. I.U. is supported by a grant from the Rising Tide Foundation. N.K.H., K.D.-R. and R.A.S. are supported by fellowships from the NHMRC. A.L.P. is supported by Cure Cancer Australia. Support from the Melanoma Institute Australia is also gratefully acknowledged. We thank the TCGA Research Network for generating some of the data sets.

AUTHOR CONTRIBUTIONS

R.A., N.Q., R.E., A.K.-P., J.J.G. and Y.S. designed the study. J.M., A.E., J.S.W., J.J.G., K.D.-R., P.J., A.L.P., N.W., G.J.M., R.A.S., N.K.H. and S.A.R. collected and analyzed the melanoma samples. S.S., R.R., J.C.L., J.K., S.B.-D. and I.U. analyzed the genetic data. R.A., R.E., S.W.-K., V.K.H., Y.H. and J.M. performed the functional experiments and analyzed the data. A.D.P. and M.Y.N. performed the structural analysis. All authors contributed to the final version of the manuscript.

COMPETING FINANCIAL INTERESTS

The authors declare no competing financial interests.

1. Siegel, R., Naishadham, D. & Jemal, A. *CA Cancer J. Clin.* **62**, 283–298 (2012).
2. Hodis, E. *et al. Cell* **150**, 251–263 (2012).
3. Krauthammer, M. *et al. Nat. Genet.* **44**, 1006–1014 (2012).
4. Krauthammer, M. *et al. Nat. Genet.* **47**, 996–1002 (2015).
5. Flaherty, K.T. *et al. N. Engl. J. Med.* **363**, 809–819 (2010).
6. Chapman, P.B. *et al. N. Engl. J. Med.* **364**, 2507–2516 (2011).
7. Lemmon, M.A. & Schlessinger, J. *Cell* **141**, 1117–1134 (2010).
8. Vivanco, I. & Sawyers, C.L. *Nat. Rev. Cancer* **2**, 489–501 (2002).
9. Sjöblom, T. *et al. Science* **314**, 268–274 (2006).
10. Vogelstein, B. *et al. Science* **339**, 1546–1558 (2013).
11. Maertens, O. & Cichowski, K. *Adv. Biol. Regul.* **55**, 1–14 (2014).
12. Miao, W., Eichelberger, L., Baker, L. & Marshall, M.S. *J. Biol. Chem.* **271**, 15322–15329 (1996).
13. Rodriguez-Viciana, P., Oses-Prieto, J., Burlingame, A., Fried, M. & McCormick, F. *Mol. Cell* **22**, 217–230 (2006).
14. Kiel, C., Verschueren, E., Yang, J.S. & Serrano, L. *Sci. Signal.* **6**, ra109 (2013).
15. Ko, L.J. & Prives, C. *Genes Dev.* **10**, 1054–1072 (1996).
16. Papa, A. *et al. Cell* **157**, 595–610 (2014).
17. Fang, J.Y. & Richardson, B.C. *Lancet Oncol.* **6**, 322–327 (2005).
18. Mann, G.J. *et al. J. Invest. Dermatol.* **133**, 509–517 (2013).
19. Jayawardana, K. *et al. Int. J. Cancer* **136**, 863–874 (2015).

ONLINE METHODS

Tumor tissues. All DNA samples used in this study were derived from metastases. Samples used for whole-exome capture were extracted from cell lines established directly from patient tumors as described previously[20]. DNA subjected to whole-genome sequencing was extracted from optimal cutting temperature (OCT)-embedded specimens as described previously[20]. Tissue was further collected and cell lines were established at the QIMR Berghofer Medical Research Institute. All cell lines were established as described previously[21], with informed patient consent under a protocol approved by the QIMR Berghofer Medical Research Institute Human Research Ethics Committee.

A subset of cell lines used in the study (108T, 55T and 76T) were derived from a panel of pathology-confirmed metastatic melanoma tumor resections collected from patients enrolled in institutional review board (IRB)-approved clinical trials at the Surgery Branch of the National Cancer Institute. Pathology-confirmed melanoma cell lines were derived from mechanically or enzymatically dispersed tumor cells, which were then cultured in RPMI-1640 supplemented with 10% FBS at 37 °C in 5% CO_2 for 5–15 passages. The C084 cell line was established at the QIMR Berghofer Medical Research Institute as described previously[21], with informed patient consent under a protocol approved by the QIMR Berghofer Medical Research Institute Human Research Ethics Committee. Cell line genotypes are given in **Supplementary Table 4**. All cell lines have tested negative for mycoplasma.

PCR, sequencing and mutational analysis. PCR and sequencing of *RASA2* were carried out as previously described[22]. Sequence traces were analyzed using the Mutation Surveyor software package (SoftGenetics). The primers used are listed in **Supplementary Table 5**.

Statistical analyses. To evaluate whether the frequency of somatic mutations was significantly higher than would be expected if the mutations were neutral, we performed the following statistical test. The null hypothesis was that the probability of a mutation at a specific base was the neutral rate of 11.4 mutations/Mb ($P = 11.4 \times 10^{-6}$). We computed a one-sided *P* value using the pbinom function in R statistical software. To determine whether the ratio of nonsynonymous to synonymous mutations observed was statistically significant, the exact binomial test was used, with an expected ratio of 2.5:1 (ref. 9). Sample size took into account a binomial distribution based on the number of base pairs sequenced for the gene of interest, the number of mutations observed and the background rate of mutation. For the background rate, we used the observed rate in the exome screen: 11.2 mutations/Mb. With this study design, there was a greater than 99% probability of identifying a gene that was mutated at a frequency of 1% or higher. All statistical calculations were performed in the R statistical environment. Further statistical analyses were performed using Microsoft Excel to generate *P* values to determine significance (two-tailed *t* test). Frameshift, nonsense and deleterious mutations were predicted by SIFT analysis.

CytoScan array processing and analysis. Samples were prepared according to Affymetrix protocols. DNA quality and quantity were ensured using Bioanalyzer (Agilent Technologies) and NanoDrop (Thermo Scientific) instruments, respectively. For DNA labeling, 200 ng of genomic DNA was used in conjunction with the Affymetrix-recommended protocol for the CytoScan HD array kit and reagents (901835). The hybridization cocktail containing fragmented and labeled DNA was incubated with the Affymetrix CytoScan HD GeneChip. Chips were washed and stained by the Affymetrix Fluidics Station using the standard format and protocols as described by Affymetrix. The probe arrays were stained with streptavidin-phycoerythrin solution (Molecular Probes), and signal was enhanced by using an antibody solution containing 0.5 mg/ml biotinylated antibody to streptavidin (Vector Laboratories). An Affymetrix GeneChip Scanner 3000 was used to scan the probe arrays; .cel files were generated from the scanned images using Affymetrix AGCC software, and .cyhd.cychp files were generated by Chromosome Analysis Suite (ChAS) version 2.1 software.

All the analyses were carried out with ChAS default parameters for loss of homozygosity and copy number state. A description of the samples used for this analysis is provided in **Supplementary Table 6**.

Construction of expression vectors for wild-type and mutant *RASA2*. Human *RASA2* cDNA (NM_006506) was cloned from HEK293T cDNA using PfuUltra II Hot-Start PCR Master Mix (Agilent Technologies) according to the manufacturer's instructions and the forward and reverse primers listed in **Supplementary Table 7**. A sequence encoding a FLAG tag at the N terminus of RASA2 was introduced during the cloning procedure. PCR products were cloned into the pCDF1-MCS2-EF1-Puro vector (Systems Biosciences) via the XbaI and NotI restriction sites. The mutation encoding p.Ser400Phe was introduced using fusion PCR site-directed mutagenesis. The mutation encoding p.Arg310* was created using an alternative reverse primer to introduce the relevant nonsense mutation (stop codon).

Immunoblotting. 501Mel, 108T and 55T cells stably expressing wild-type or mutant FLAG-RASA2 or with empty vector were gently washed two times in PBS and then lysed using 1.0 ml of 1% NP-40 lysis buffer (1% NP-40, 50 mM Tris-HCl, pH 7.5, 150 mM NaCl, Complete Protease Inhibitor tablet, EDTA-free (Roche), 1 μM sodium orthovanadate, 1 mM sodium fluoride and 0.1% β-mercaptoethanol) per T75 flask for 20 min on ice. Lysed cells were scraped and transferred into a 1.5-ml microcentrifuge tube. Extracts were centrifuged for 10 min at 20,000*g* at 4 °C. Proteins (50 μg/lane) were resolved by 10% SDS-PAGE and transferred to nitrocellulose membranes (Bio-Rad). Immunoblots were probed with the following antibodies: anti-FLAG (M2) (F7425, Sigma-Aldrich) and antibody to GAPDH (MAB374, Millipore). RAS-GTP levels were determined using a RAS Activation Assay kit (EMD Millipore). Every RAS-GTP assay was performed twice.

Pooled stable expression. To produce lentivirus, the *RASA2* constructs were cotransfected into HEK293T cells seeded at 2.5×10^6 cells per T75 flask with the pVSV-G and pFIV-34N helper plasmids (kind gifts from T. Waldman, Georgetown University) using Lipofectamine 2000 (Life Technologies) as described by the manufacturer. Virus-containing medium was collected 60 h after transfection, filtered, aliquotted and stored at −80 °C.

501Mel, 55T and 108T cells were grown in RPMI-1640 supplemented with 10% FBS (HyClone). Lentivirus for RASA2 (wild type, Arg310* and Ser400Phe) and empty vector control were used to infect the cells as previously described[23]. Stable expression of the RASA2 proteins (wild type and mutant) was determined by SDS-PAGE analysis followed by immunoblotting with antibodies to FLAG and GAPDH to show equivalent expression among pools.

siRNA depletion of endogenous *RASA2*. Two siRNAs specific to human *RASA2* (ON-TARGETplus) were designed using the siRNA design program for human *RASA2* and were purchased from Dharmacon (Thermo Fisher Scientific). The sequences of the two siRNAs used to transiently deplete *RASA2* in malignant melanoma cell lines are provided in **Supplementary Table 8**. Using DharmaFECT Transfection Reagent 1 (specific for siRNA), melanoma cell lines were transfected with 50 nM ON-TARGET siRNA in the presence of OptiMEM-I medium (Life Technologies). Cells were incubated for 72 h after transfection before checking RAS-GTP levels using the RAS Activation Assay kit.

Lentiviral shRNA. All shRNA expression constructs were obtained from Open Biosystems. Lentiviral stocks were prepared as previously described[22]. NIH3T3 cells were infected with lentivirus encoding shRNA for each condition (vector control and two independent shRNAs specific to mouse *Rasa2*) and selected as previously described[22]. The shRNA constructs used in this study were sh50 (TRCN0000034350) and sh51 (TRCN0000034351).

doi:10.1038/ng.3427

Three-dimensional RAS-RASA2 model prediction. The complex of human HRAS bound to the GTPase-activating domain of the human GAP p120^{GAP} (GAP-334; 1WQ1, Protein Data Bank (PDB))[24] was used as a template to create both RASA2 RasGAP domain and Mg^{2+}-NRAS-GTP models (1WQ1 chain R, HRAS). The GAP-334 sequence present in the PDB file was shorter than that of RASA2, but it covered the binding interface, was bound to RAS and had high similarity to the queried RASA2 sequence. Sequence alignment and homology modeling were performed with Prime (version 4.0, Schrödinger). The initial X-ray structure 1WQ1 contains the substrate GDP-AlF3 bound to HRAS. The AlF3 molecule, which is thought to mimic the γ-phosphate moiety of GTP[24], was manually replaced by a γ-phosphate group bound to GDP.

The hydrogen atoms and side-chain orientations of the GTP-NRAS-RASA2 complex were optimized with the Protein Preparation Wizard tool from Schrödinger at physiological pH. Side chains were refined with the Predict Side Chains tool available in Prime. The energies for both the GTP-NRAS–wild-type RASA2 and GTP-NRAS–Ser400Phe RASA2 complexes were then minimized to a derivative convergence of 0.05 kJ/mol-Å using the Polak-Ribiere Conjugate Gradient (PRCG) minimization algorithm, the OPLS2005 force field and the GB/SA water solvation model implemented in MacroModel (version 10.8, Schrödinger): the finger loop was free to move, a shell of 5 Å around the loop minimized applying a force constant of 200 kJ/mol-Å^2 and another shell of 5 Å with a constant force of 300 kJ/mol-Å^2.

Proliferation assays. To examine cell growth, melanoma cell lines (501Mel, 55T and 108T) stably infected with vector or vector encoding wild-type, Arg310* or Ser400Phe RASA2 were seeded in six replicates in 96-well plates at 200–2,000 cells per well and incubated for 7–17 d. Samples were analyzed every 48 h by lysing cells in 50 µl of 0.2% SDS/well and incubating for 2 h at 37 °C before the addition of 150 µl/well of SYBR Green I solution (1:750 dilution of SYBR Green I (Invitrogen-Molecular Probes) in distilled water).

Soft agar assays. 501Mel, 108T and 55T pooled RASA2-expressing clones were plated in four replicates at 1,000 cells/well in top plugs consisting of sterile 0.33% Bacto Agar (BD) and 2.5% FBS in a 24-well plate. The lower plug contained sterile 0.5% Bacto Agar and 2.5% FBS. After 1 week, colonies were counted.

Migration assays. Blind well chemotaxis chambers with a 13-mm diameter and polycarbonate filters with an 8-mm pore size (Costar Scientific) were used. Cells (2×10^5) suspended in serum-free medium were added to the upper chamber. Full medium containing 10% FBS was placed in the lower chamber. Assays were carried out at 37 °C in 5% CO_2. After incubation (12–24 h), the upper surface of the filter was freed of cells using a cotton swab. Cells that passed through the filter to the bottom side were fixed in methanol and then stained by Geimsa. Each triplicate assay was performed three times. Migrating cells were counted without knowledge of sample identity in ten representative light-microscopy fields.

RASA2 immunohistochemistry. RASA2 immunohistochemistry was performed on AJCC stage III melanoma tumor microarrays (TMAs). Staining was performed using rabbit polyclonal antibody to RASA2 from Sigma-Aldrich (HPA035375) on a DAKO immunohistochemistry autostainer using the DAKO EnVision FLEX+ detection system (K8002) with DAB as the chromogen (DAKO, K3467), according to the manufacturer's instructions (high-pH antigen retrieval; primary antibody dilution of 1:100 for 60 min). The resultant immunohistochemistry signal was predominantly cytoplasmic. Cases were scored by the percentage of cytoplasm-positive tumor cells (0–100%) and overall tumor staining intensity (0–4). Typically, in positive samples, there was homogeneous staining across 100% of the tumor cells. The intensity of staining varied between patients and ranged from negative (intensity = 0) to weakly positive (intensity of 1 or 2) and strongly positive (intensity of 3 or 4). The Kaplan-Meier graph represents negative (intensity = 0) versus positive (intensity = 1–4) cases.

Tumor microarray cohort description. Samples eligible for this TMA were obtained at the Melanoma Institute Australia Biospecimen Bank from AJCC stage III (lymph node) metastatic melanoma specimens in which macroscopic tumor was observed, from patients believed to be without distant metastases at the time of tumor banking on the basis of clinical examination and computerized axial tomographic scanning of the brain, chest, abdomen and pelvis. Key covariates were balanced in this cohort to permit survival analysis. These samples were used to derive **Figure 1f**.

20. Wei, X. *et al. Nat. Genet.* **43**, 442–446 (2011).
21. Dutton-Regester, K. *et al. Oncotarget* **5**, 2912–2917 (2014).
22. Palavalli, L.H. *et al. Nat. Genet.* **41**, 518–520 (2009).
23. Solomon, D.A. *et al. Cancer Res.* **68**, 10300–10306 (2008).
24. Scheffzek, K. *et al. Science* **277**, 333–338 (1997).